Accepted Manuscript

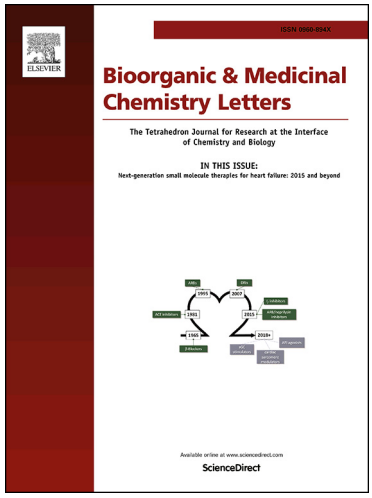

Discovery of novel quinoline sulphonamide derivatives as potent, selective and orally active RORγ inverse agonists

Jérôme Amaudrut, Maria A. Argiriadi, Martine Barth, Eric C. Breinlinger, Didier Bressac, Pierre Broqua, David J. Calderwood, Mohamed Chatar, Kevin P. Cusack, Stephen B. Gauld, Sébastien Jacquet, Rajesh V. Kamath, Michael E. Kort, Valérie Lepais, Jean-Michel Luccarini, Philippe Masson, Christian Montalbetti, Laurent Mounier, Dominique Potin, Olivia Poupardin, Sylvie Rouaud, Luc Spitzer, Craig D. Wallace

PII: S0960-894X(19)30301-4
DOI: https://doi.org/10.1016/j.bmcl.2019.05.015
Reference: BMCL 26435

To appear in: *Bioorganic & Medicinal Chemistry Letters*

Received Date: 5 March 2019
Revised Date: 2 May 2019
Accepted Date: 7 May 2019

Please cite this article as: Amaudrut, J., Argiriadi, M.A., Barth, M., Breinlinger, E.C., Bressac, D., Broqua, P., Calderwood, D.J., Chatar, M., Cusack, K.P., Gauld, S.B., Jacquet, S., Kamath, R.V., Kort, M.E., Lepais, V., Luccarini, J-M., Masson, P., Montalbetti, C., Mounier, L., Potin, D., Poupardin, O., Rouaud, S., Spitzer, L., Wallace, C.D., Discovery of novel quinoline sulphonamide derivatives as potent, selective and orally active RORγ inverse agonists, *Bioorganic & Medicinal Chemistry Letters* (2019), doi: https://doi.org/10.1016/j.bmcl.2019.05.015

Graphical Abstract

To create your abstract, type over the instructions in the template box below.
Fonts or abstract dimensions should not be changed or altered.

Discovery of novel quinoline sulphonamide derivatives as potent, selective and orally active RORγ inverse agonists

Leave this area blank for abstract info.

Jérôme Amaudrut[a], Maria A. Argiriadi[b], Martine Barth[a], Eric C. Breinlinger[b], Didier Bressac[a], Pierre Broqua[a], David J. Calderwood[c], Mohamed Chatar[a], Kevin P. Cusack[b], Stephen B. Gauld[d], Sébastien Jacquet[a], Rajesh V. Kamath[c], Michael E. Kort[d], Valérie Lepais[a], Jean-Michel Luccarini[a], Philippe Masson[a], Christian Montalbetti[a], Laurent Mounier[a], Dominique Potin[a, *], Olivia Poupardin[a], Sylvie Rouaud[a], Luc Spitzer[a], Craig D. Wallace[c]

[a]Inventiva, 50 rue de Dijon, 21121 Daix, France
[b]AbbVie, 381 Plantation Street, Worcester, MA 01605, USA
[c]AbbVie, 100 Research Drive, Worcester, MA 01605, USA

Bioorganic & Medicinal Chemistry Letters
journal homepage: www.elsevier.com

Discovery of novel quinoline sulphonamide derivatives as potent, selective and orally active RORγ inverse agonists

Jérôme Amaudrut[a], Maria A. Argiriadi[b], Martine Barth[a], Eric C. Breinlinger[b], Didier Bressac[a], Pierre Broqua[a], David J. Calderwood[c], Mohamed Chatar[a], Kevin P. Cusack[b], Stephen B. Gauld[d], Sébastien Jacquet[a], Rajesh V. Kamath[c], Michael E. Kort[d], Valérie Lepais[a], Jean-Michel Luccarini[a], Philippe Masson[a], Christian Montalbetti[a], Laurent Mounier[a], Dominique Potin[a, *], Olivia Poupardin[a], Sylvie Rouaud[a], Luc Spitzer[a], Craig D. Wallace[c]

[a]*Inventiva, 50 rue de Dijon, 21121 Daix, France*
[b]*AbbVie, 381 Plantation Street, Worcester, MA 01605, USA*
[c]*AbbVie, 100 Research Drive, Worcester, MA 01605, USA*
[d]*AbbVie, 1 North Waukegan Road, North Chicago, IL 60064, USA*

ARTICLE INFO

Article history:
Received
Revised
Accepted
Available online

Keywords:
RORγt inverse agonist
Th17 cells
IL-17
Nuclear hormone receptor
SAR

ABSTRACT

A high-throughput screen against Inventiva's compound library using a Gal4/RORγ-LBD luciferase reporter gene assay led to the discovery of a new series of quinoline sulphonamides as RORγ inhibitors, eventually giving rise to a lead compound having an interesting *in vivo* profile after oral administration. This lead was evaluated in a target engagement model in mouse, where it reduced IL-17 cytokine production after immune challenge. It also proved to be active in a multiple sclerosis model (EAE) where it reduced the disease score. The synthesis, structure activity relationship (SAR) and biological activity of these derivatives is described herein.

* Corresponding author. e-mail: dominique.potin@inventivapharma.com

RORγ (Retinoic acid-related Orphan Receptor γ) is a nuclear receptor from a family consisting of three members (together with RORα and RORβ).[1] RORα which is widely expressed, plays a role in lipid regulation in the liver and regulates circadian rhythm in the CNS. RORβ is mainly expressed in the cerebral cortex and the retina where it plays a role during development. RORγ is expressed in thymus, skeletal muscles, skin, adipose tissue and kidney ; it has an isoform called RORγt which is identical in sequence with the exception of a few missing amino acids on the *N*-terminal side. RORγt is expressed in immune cells such as Th17 and γδTcells.[2] The ligand binding domain (LBD) of the three RORs is highly similar making the obtaining of selective compounds quite challenging. This binding site is highly lipophilic especially in the vicinity of Helix 10 (Fig. 1),[3] the only polar part being close to two arginine residues (Arg364 and Arg367). This polar area has an opening to the solvent and water molecules are found in this region in many published RORγ XRay structures.[4]

RORγt is a key player in the IL-17 pathway. It is involved in the differentiation of naive Tcells into Th17[5] where both RORα and RORγ are highly expressed. It is also involved in the synthesis of proinflammatory cytokines such as IL-17a, IL-17f and IL-22.

Anti IL-17 antibodies such as secukinumab have shown the interest of blocking IL-17 for treating psoriasis[6] and psoriatic arthritis.[7] A small molecule RORγt inverse agonist would, in theory, have an advantage over the antibody by blocking the cascade upstream at two different stages, making it a good candidate in the treatment of IL-17/Th17 mediated autoimmune diseases.[8] Such an interesting target has drawn attention from many research groups.[9]

A high throughput screen (HTS) was run against Inventiva's collection (248k compounds) looking for inverse agonist activity in a luciferase reporter gene assay using a chimeric receptor Gal4 DNA-binding domain (DBD)- human RORγ LBD transiently transfected in COS-7 cells. T0901317 (Fig. 2) was used for normalization as giving 100% antagonist response in all *in vitro* experiments.[10] Although the hit rate was quite low (0.17%), relatively potent hits were identified including a small series of quinoline sulphonamides exemplified by compound **1** which displays micromolar activity (Fig. 2). Herein we report modifications to this structure, leading to potent and selective RORγ inverse agonists which inhibited IL-17a production in a cellular assay. These efforts culminated in the identification of a compound that is orally active in a mouse experimental autoimmune encephalomyelitis (EAE) model, a preclinical model for multiple sclerosis.

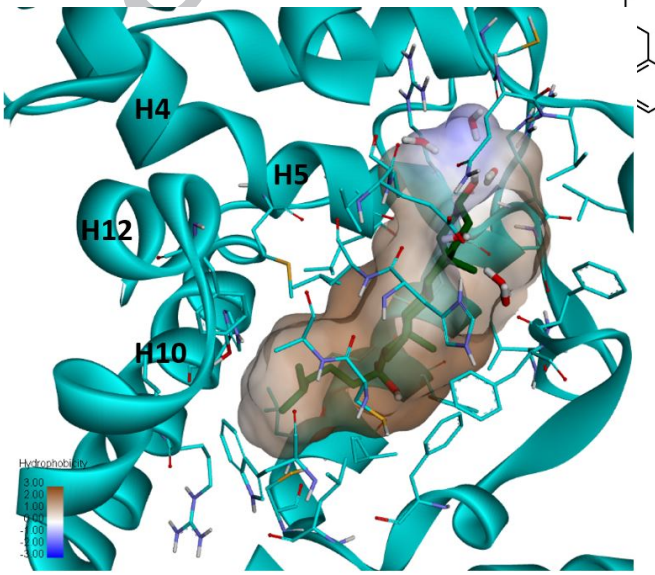

Figure 1. RORγ LBD bound to 20-hydroxycholesterol in green (PDB: 3KYT) in agonist conformation, colored according to lipophilicity (from brown: highly lipophilic to blue: hydrophilic).

During the optimization phase three different assays have been routinely used to characterize the compounds. The first one, the Gal4/RORγ-LBD luciferase reporter gene assay, is similar to the one used during the HTS campaign. The compounds were then evaluated in an IL-17a secretion inhibition assay in human Th17 cells. Finally the selectivity vs the other ROR isoforms was evaluated in a coactivator recruitment assay using alphascreen™ technology. As compounds were very selective for RORγ vs RORβ (RORβ EC_{50} > 30μM) only the selectivity vs RORα is indicated. This data is reported in the subsequent SAR (Structure Activity Relationship) tables.

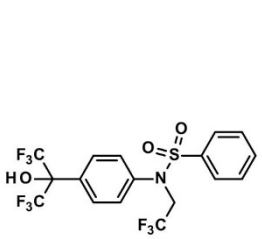

T0901317

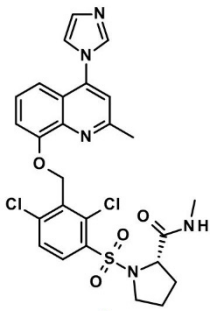

1

hRORγ EC_{50} = 1.4 μM (107%)

Figure 2. Structure of reference and hit compounds.

Our first modification of the compounds was to look at the quinoline substitution (Table 1). Activity increased with the size of the substituent at position 2, however with a loss of selectivity towards RORα. Introduction of polar groups in this position - alcohols, ether, amines - was not tolerated (data not shown). Replacement of the imidazole in 4-position by a trifluoromethyl group improved potency in the GAL-4 assay but came with loss in human and mouse microsomal stability.

Table 1
SAR around quinoline substitution.

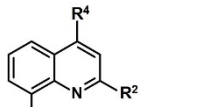

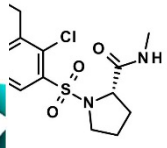

Compd.	R^2	R^4	hRORγ EC_{50} [a] (μM) (%eff)[b]	IL17 inhibition EC_{50} [c] (μM) (%eff)[b]	Selectivity [d]	hClint,u [e] (L/h/kg)	mClint,u [e] (L/h/kg)
T0901317			1.08 (100%)	0.93 (100%)	418		
1	Me		1.36 (107%)	3.00 (72%)	49	2	16
2	iPr		0.52 (113%)	nd	13	2	8
3	CF_3		0.17 (106%)	3.32 (77%)	12	1	8
4	Me	CF_3	0.25 (108%)	0.21 (89%)	32	15	83
5	Et	CF_3	0.35 (105%)	0.21 (108%)	23	18	77
6	iPr	CF_3	0.17 (111%)	0.77 (97%)	9	30	98

[a] Gal4/RORγ-LBD luciferase reporter gene assay. [b] Percent efficacy represents maximum inhibition (100% being the maximum activity of T0901713). [c] Inhibition of IL-17 secretion in human Th17 cells. [d] Selectivity in the alphascreen™ assay expressed as ratio of RORα EC_{50}/RORγ EC_{50}. [e] Human and mouse microsomal unbound clearance. All assay results are reported as the geometric mean of at least two separate runs.

Table 2 outlines the SAR effort on the dichlorosulfonamide moiety. Removal of the chlorine atoms in the central ring was deleterious to the activity (compounds **4** and **7**, Table 2). These two chlorine atoms are locking the quinoline ring in a position perpendicular to the plane of the dichlorophenyl ring. The energy barriers of rotation around the phenyl C_{arom}-C and benzyl C-O bonds have both been calculated to be ~ 5 kcal.mol^{-1} using the OPLS3e force field.[11] Such a spatial arrangement can be seen for example in the published structure of 2,6-dichlorobenzyl 4-nitrophenyl ether (Fig. 3).

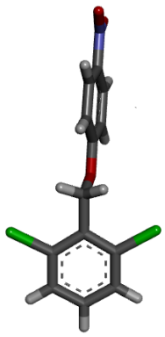

Figure 3. X-Ray structure of 2,6-Dichlorobenzyl 4-nitrophenyl ether (CSD: VAFBIN).

Switching from a secondary methylamide **4** to a primary amide **8** decreased activity and microsomal stability, but with an improved selectivity for RORγ. The carboxylic derivative **9** is significantly less potent. The methoxy ether derivative **11** is equivalent to compound **4** with a slightly lower potency in inhibition of IL-17 secretion (72% *vs* 86%). Unsubstituted pyrrolidine and piperidine derivatives **13** and **14** are less active. Introduction of polar groups such as in alcohol **15** restores the activity. From these initial SAR observations, it was hypothesized that the quinoline part of the molecule was sitting in the lipophilic area close to Helix H10 and that the sulphonamide moiety was pointing in the polar area close to Arg364 and Arg367. The more polar carboxylic acid **9** seemed not to be tolerated in this slightly polar environment as its activity dropped significantly. This could result from a solvation issue. Although polar groups in general were predicted to be fitting well in the polar area close to Arg364 and Arg367, the actual prediction of activity based on docking experiments proved to be quite challenging due to the presence of many water molecules in this portion of the LBD and the difficulty to accurately evaluate their contribution to the binding of the ligand. We thus had to rely on a library approach where the position of the polar group was explored in a systematic way using different chain lengths and orientations. The initially found *N*-methylprolinamide group remained one of the best substituent on the sulphonamide.

Table 2
SAR around phenyl linker and sulphonamide substitutions.

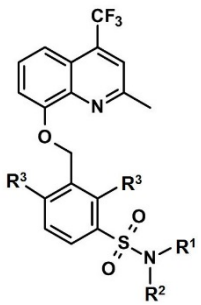

Compd.		R^3	hRORγ EC_{50} [a] (μM) (%eff)[b]	IL17 inhibition EC_{50} [c] (μM) (%eff)[b]	Selectivity [d]	hClint,u [e] (L/h/kg)	mClint,u [e] (L/h/kg)
4		Cl	0.25 (108%)	0.21 (86%)	32	15	83
7		H	>10 (30%)	nd	nd	3	46
8		Cl	0.44 (108%)	0.47 (88%)	> 380	10	756
9		Cl	1.39 (96%)	nc (64%)	> 190	0.5	0.8
10		Cl	0.96 (111%)	0.83 (93%)	22	15	98
11		Cl	0.16 (102%)	0.16 (72%)	> 70	27	97
12		Cl	0.91 (105%)	nc (93%)	nd	10	52
13		Cl	0.81 (59%)	0.30 (67%)	> 45	14	58
14		Cl	0.90 (77%)	nd	> 40	14	60
15		Cl	0.39 (96%)	nc (76%)	> 200	22	65
16		Cl	0.22 (84%)	nd	> 7	19	56
17		Cl	0.76 (103%)	nc (90%)	> 190	26	103

[a] Gal4/RORγ-LBD luciferase reporter gene assay. [b] Percent efficacy represents maximum inhibition (100% being the maximum activity of T0901713). [c] Inhibition of IL-17 secretion in human Th17 cells. [d] Selectivity in the alphascreen™ assay expressed as ratio of RORα EC_{50}/RORγ EC_{50}. [e] Human and mouse microsomal unbound clearance. All assay results are reported as the geometric mean of at least two separate runs.

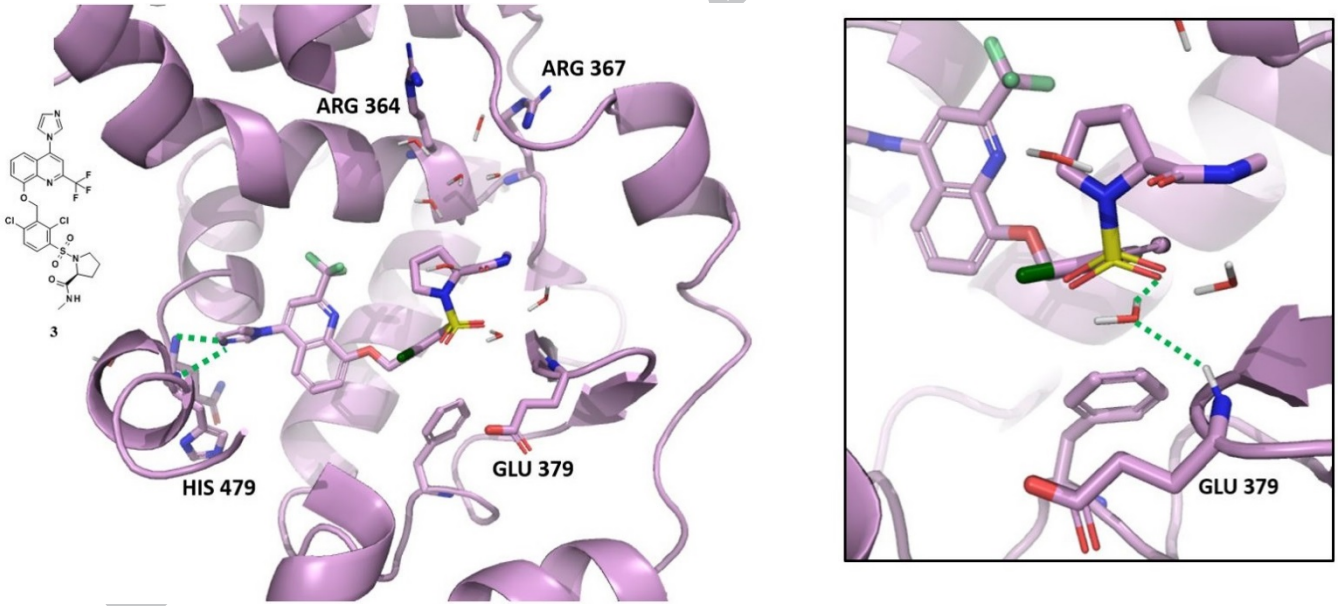

Figure 4. Crystal structure of human RORγ LBD bound to compound **3** (PDB: 6Q2W), with zoom on the water network in the sulphonamide region.

A co-crystal structure of RORγ LBD with compound **3** was obtained and confirmed our docking hypothesis (Fig. 4). The imidazole moiety makes two hydrogen bonds with the backbone NH of Gln478 and His479. The sulphonyl group is hydrogen bound to the backbone NH of Glu379 via a water molecule. The amide group borne by the proline is pointing towards the solvent. There are many water molecules filling the pocket in the proximity of Arg364 and Arg367. As expected the ligand has a conformation where the plane of the quinoline is perpendicular to the one from the dichlorophenyl central ring.

In its agonist conformation, the helix H12 of RORγ is locked in a position allowing the recruitment of the co-activators which are required for the transcription to occur. The triad of essential amino acids for the stabilization of RORγ in this conformation are His479, Tyr502 and Trp317. Key interactions are a hydrogen bond between His479 and Tyr502, and an edge to face π-π interaction between Tyr502 and Trp317. Any disturbance of this spatial arrangement is very likely to result in decreased agonist response and a shift towards an antagonist conformation. This is the case when compound **3** binds to the pocket. As shown in Figure 5, His479 residue is pushed away from its agonist conformation, the ligand also induces a kink in Helix 10 which in turn greatly disturbs the organization of H11 and H12. The latter is no longer resolved in the crystal structure, probably because of its high mobility caused by the impossibility to reach its stable agonist conformation. Interestingly, two hydrogen bonds are observed between the ligand and the backbone nitrogen atoms of residues Gln478 and His479. It is expected that these interactions stabilize

the kinked conformation of helix 10 and contribute to the antagonist character of the ligand.

With the prolinamide in place, a new set of compounds was prepared trying to modify the imidazole on the quinoline 4-position (Table 3). The 3- and 4-pyridyl derivatives **23** and **24** were quite interesting in terms of activity but with a moderate RORγ/RORα selectivity. The 4-imidazolyl substitution of **18** increased significantly this selectivity to 133 fold in favor of RORγ. With a 2-isopropyl group, the activity was increased. Here again the 4-pyridyl derivative **27** was quite active and poorly selective, whereas the 4-imidazolyl derivative **29** gave a comparable activity with a very good selectivity (>2500 x) against RORγ. This compound was chosen for further *in vivo* characterization.

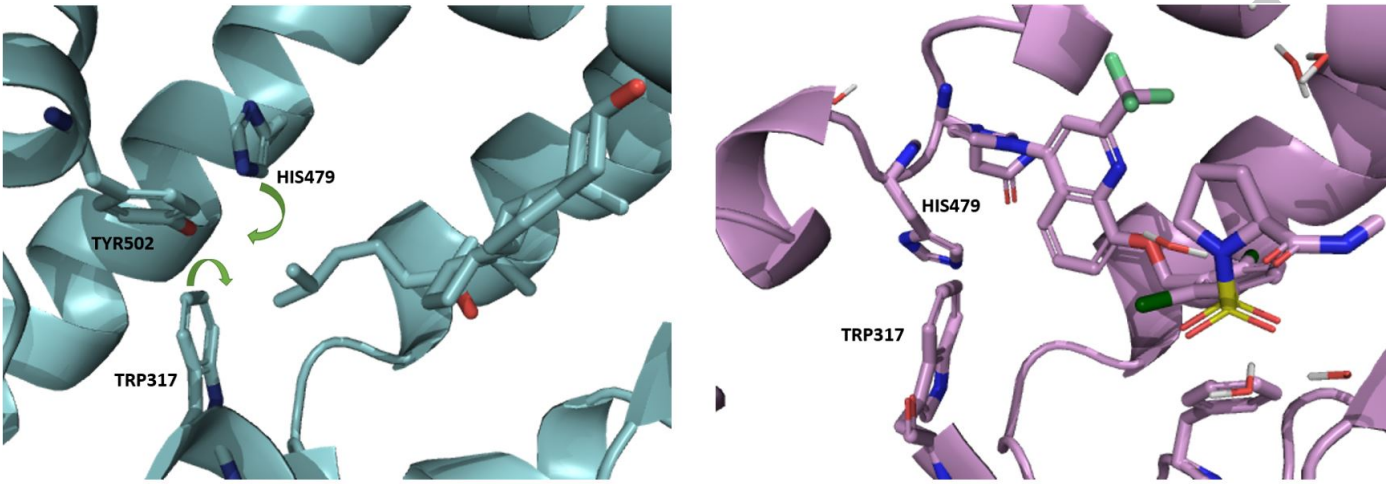

Figure 5. Switch from agonist to inverse agonist conformation: RORγ LBD in agonist conformation as bound to 20-hydroxycholesterol (blue gray, PDB: 3KYT) and in inverse agonist conformation when bound to compound **3** (pink, PDB : 6Q2W).

Table 3
SAR around quinoline substitution.

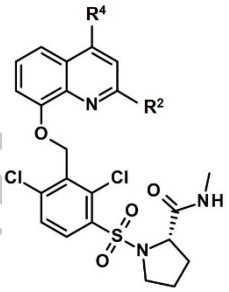

Compd.	R^2	R^4	hRORγ EC_{50} [a] (μM) (%eff)[b]	IL17 inhibition EC_{50} [c] (μM) (%eff)[b]	Selectivity [d]	hClint,u [e] (L/h/kg)	mClint,u [e] (L/h/kg)
1	Me		1.36 (107%)	3.00 (72%)	49	2	16
18	Me		1.51 (104%)	1.39 (78%)	133	2	7
19	Me		>10 (100%)	nt	5	7	55
4	Me	CF3	0.25 (108%)	0.21 (89%)	32	15	83
20	Me	Ph	0.32 (109%)	0.89 (108%)	10	nt	nt
21	Me	OBn	0.88 (114%)	nt	32	28	109
22	Me		1.66 (106%)	2.07 (73%)	> 240	11	44
23	Me		0.10 (113%)	1.01 (87%)	16	14	42
24	Me		0.63 (111%)	nc (91%)	81	13	33

25	iPr		0.52 (113%)	nt	13	2	8
26	iPr	CF_3	0.17 (111%)	0.77 (97%)	9	30	98
27	iPr		0.22 (108%)	1.83 (104%)	5	20	38
28	iPr	OBn	0.94 (109%)	>5 (117%)	7	40	73
29	iPr		0.22 (114%)	0.15 (92%)	> 2500	2	6

[a] Gal4/RORγ-LBD luciferase reporter gene assay. [b] Percent efficacy represents maximum inhibition (100% being the maximum activity of T0901713). [c] Inhibition of IL-17 secretion in human Th17 cells. [d] Selectivity in the alphascreen™ assay expressed as ratio of RORα EC_{50}/RORγ EC_{50}. [e] Human and mouse microsomal unbound clearance. All assay results are reported as the geometric mean of at least two separate runs.

Synthesis of compound **29** started with the condensation of o-anisidine **30** with β-ketoester **31** in polyphosphoric acid (PPA) (Fig. 6). To get a reasonably good yield in this reaction, it was essential to proceed with a two-step heating, starting with a plateau at 110°C before increasing to 150°C.[12] Chlorination followed by demethylation yielded chloroquinolinol **33**. Protection of the phenol with a benzyl group and subsequent conversion of the chloro to the pinacol boronate derivative **34** was realized with a quantitative yield. The imidazolyl group was then installed through a Suzuki coupling reaction under microwave irradiation. Debenzylation was then performed using ammonium formate as a source of hydrogen to deliver quinolinol **37**. The southern part of the molecule **40** was prepared using a previously reported procedure[13] and was condensed under basic conditions with quinolinol **37**. Ester hydrolysis followed by an amide coupling with methylamine completed the synthesis of compound **29**.

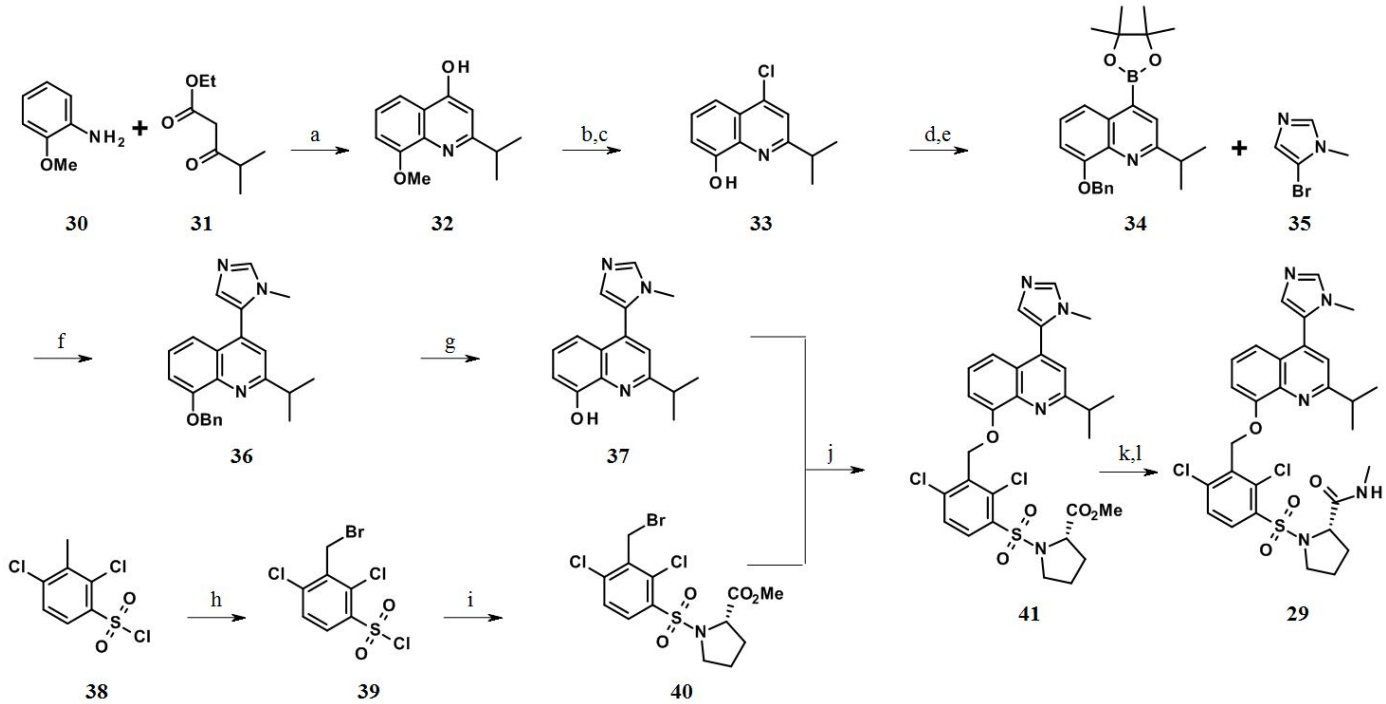

Figure 6. Synthesis of compound **29**. a) PPA, 110°C then 150°C, 30% ; b) $POCl_3$, PCl_5, 120°C, 33% ; c) $AlCl_3$, toluene reflux, 89% ; d) BnBr, K_2CO_3, DMF, 100% ; e) bis(pinacolato)diboron, $Pd(OAc)_2$, dioxane, 110°C, 99% ; f) $Pd(PPh_3)_4$, Na_2CO_3, dioxane, H_2O, microwave, 60% ; g) ammonium formate, Pd/C, MeOH reflux, 96% ; h) NBS, benzoyl peroxide, CCl_4 reflux, 47% ; i) (*S*)-Proline methyl ester HCl, Et_3N, CH_2Cl_2, 0°C, quant. ; j) K_2CO_3, DMF, 49% ; k) LiOH, THF, H_2O, 99% ; l) $MeNH_2$, EDCI HCl, HOBt, CH_2Cl_2, 77%.

Compound **29** was evaluated in mouse PK at 10 mg/kg po and 1 mg/kg iv (Table 4).

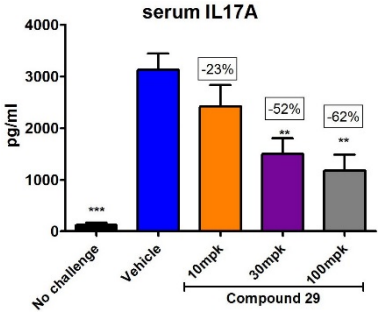

Table 4
PK parameters of compound **29** after administration in mouse (iv: 1 mg/kg, po: 10 mg/kg)

PK parameter	Data
po Tmax	0.25 h
po Cmax	3324 ng/mL
po AUC_{last}	3903 ng*h/mL
Clp,u	97 L/h/kg
Clp	1.65 L/h/kg
iv $t_{1/2}$	0.16 h
Bioavailability, F	64 %

po = suspension in 1% Methylcellulose 400cp + 0.1% Poloxamer 188 ; iv = Cremophor EL 2% in 0.9% NaCl solution

Compound **29** was first evaluated *in vivo* in a mechanistic model where mice were first immunized with a mixture of mouse MOG35-55 peptide (Myelin Oligodendrocyte Glycoprotein) and PTX (pertussis toxin). After 5 days, the test compound was administered 45 minutes before a challenge with anti-CD3. Two hours later, circulating cytokines were measured (Fig. 7). As expected for a RORγ inverse agonist, compound **29** had a significant dose- dependent effect on Th17 cytokines (IL-17a, IL-17f, and IL-22 to a lesser extent) starting from the dose of 30 mg/kg. The effect on Th1 cytokines (IFNγ, IL2 and TNFα) and on Th2 cytokines (IL-6 and IL-10) were non-significant (see Supplementary Data).

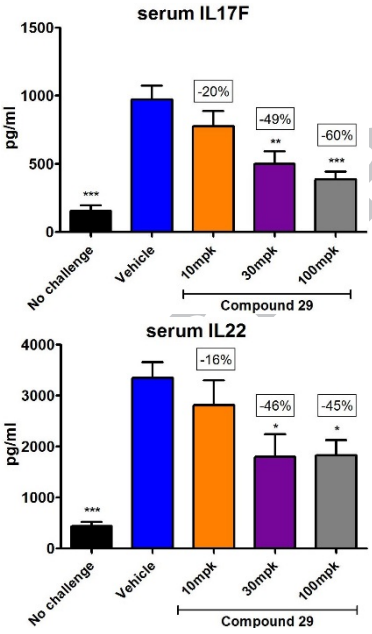

Figure 7. Effect of compound **29** on anti-CD3 induced cytokines production in mice. Compound was orally administered as a suspension in methyl cellulose 400cp + 1% poloxamer. Global p value<0.0001, Dunnett post test ; * p value<0.05 vs Vehicle ; ** p value<0.01 vs Vehicle ; *** p value <0.001 vs Vehicle.

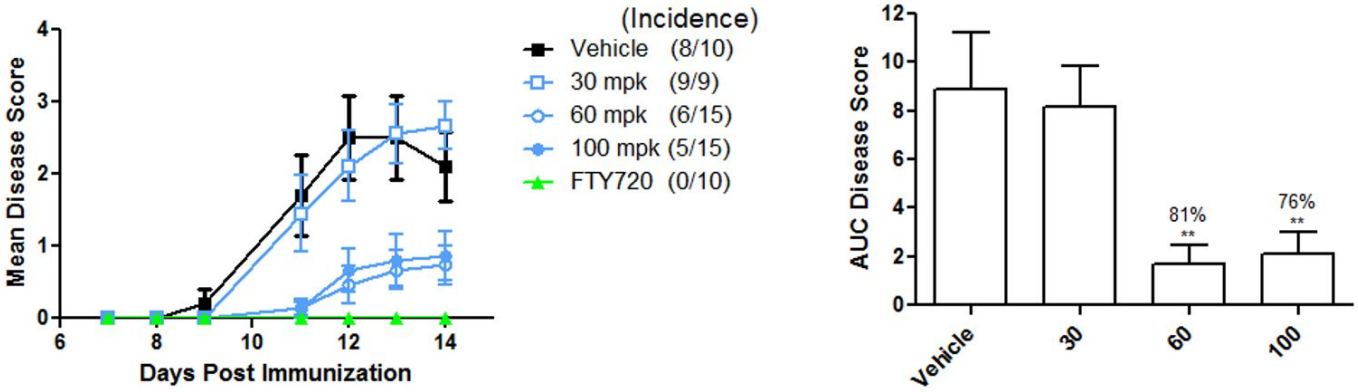

Figure 8. Effect of compound **29** in PLP-induced EAE model in mice. Compound was administered p.o. as a suspension in water in the presence of 0.1% anti-foam (w/w).

Compound **29** was then evaluated in an EAE model in mice. The mice were immunized with the encephalitogenic peptide of proteolipid protein (PLP139-151), a major myelin component. In this model, mice developed an ascending paralysis 10 to 12 days post-immunization. The compound was administered b.i.d. starting from the immunization. The animals were scored using a 5- point scoring system (0: normal ; 1: loss of tail tone ; 2: irregular gait, 3: partial hind limb paralysis, 4: total hind limb paralysis, 5: moribund). The S1P agonist fingolimod (FTY720) was used as a positive control in this experiment. Compound **29** given orally b.i.d. at 60 and 100 mg/kg p.o inhibited disease onset by 81 and 76%, respectively (Fig. 8).

For further developing compound **29**, an ascending dose PK study was performed in mice at 10, 30 and 100 mg/kg (Table 5 and Fig. 9). There was a dose proportional increase of Cmax with a slower absorption at 100 mg/kg (from 0.25 h to 3 h). A more than dose proportional increase of exposure was observed when increasing the dose from10 mg/kg up to 100 mg/kg (giving a 58 fold increase instead of the expected 10 fold), probably due to elimination saturation (increase of $t_{1/2}$ with the dose). Slower elimination of compound **29** could be due in part to high CYP3A4 inhibition (CYP inhibition at 1µM : 3A4 (99%), 2C9 (100%)), as compound **29** is metabolized mostly by this cytochrome (fraction metabolized : 3A4 (87%), 2C9 (6%)). This inhibition is very likely linked to the presence of the imidazole. Imidazoles have indeed been extensively reported to bind to the heme portion of the CYP.[14] Introduction of bulky alkyl groups on the imidazole removed the CYP 3A4 inhibition but at the cost of RORγ activity.

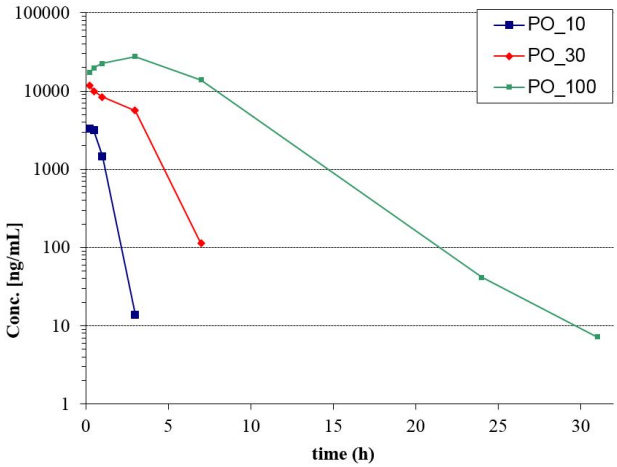

Figure 9. Ascending dose PK profile of compound **29** in mice.

Table 5.
Ascending dose PK of compound **29** in mice.

Dose po (mg/kg)	10	30	100
Tmax (h)	0.25	0.25	3
Cmax (ng/mL)	3324	11754	27541
Cmax ratio	1	3.5	8.3
Oral AUC_{last} (ng*h/mL)	3903	34186	269552
Oral AUC_{last} ratio	1	8.8	58
po $t_{1/2}$ (h)	< 1	1	2.2

Compound administered as a suspension in 1%Methylcellulose 400cp + 0.1% Poloxamer

In summary, we have identified a novel series of benzyloxyquinoline sulphonamide RORγ inhibitors. They induce the switch from an agonist to an inverse agonist structure through the combination of a steric clash with key His479 and two hydrogen bonds between the ligand and the protein backbone at the beginning of helix H11 (as observed in its co-crystal structure). Optimization of this series led to compound **29** which dose dependently reduced secretion of pro-inflammatory cytokines IL-17a and IL-17f in mice treated with MOG after oral administration. Compound **29** was also active in an EAE mouse model demonstrating the potential use of RORγ inverse agonists in the treatment of Th17-related autoimmune diseases. The good oral exposure obtained with this compound could be mostly due to CYP3A4 inhibition by compound **29** itself. As all attempts to get rid of this inhibition proved to be unsuccessful, it was decided to redesign this series of sulphonamide based RORγ inverse agonists.

Acknowledgements:

We thank Fabrice Ciesielski (Novalix) for the resolution of the crystal structure of compound **3** in RORγ LBD.

References and notes

1. (a) Jetten, A.M. *Nucl. Recept. Signal.* **2009**, *7*, e003. DOI: 10.1621/nrs.07003.
   (b) Cook, D.N.; Kang, H.S.; Jetten, A.M. *Nucl. Receptor Res.* **2015**, *2*, 101185. DOI: 10.11131/2015/101185.
2. Sutton, C.E.; Mielke, L.A.; Mills, K.H. *Eur. J. Immunol.* **2012**, *42*, 2221. DOI: 10.1002/eji.201242569.
3. Jin, L.; Martynowski, D.; Zheng, S.; Wada, T.; Xie, W.; Li, Y. *Mol. Endocrinol.* **2010**, *24*, 923. DOI: 10.1210/me.2009-0507.
4. See Supplementary Data for examples of RORγ LBD showing water molecules in the polar area close to arginines.
5. Ivanov, I.I.; McKenzie, B.S.; Zhou, L.; Tadokoro, C.E.; Lepelley, A.; Lafaille, J.J.; Cua, D.J.; Littman, D.R. *Cell*, **2006**, *126*, 1121. DOI: 10.1016/j.cell.2006.07.035.

6. Papp, K.A.; Langley, R.G.; Sigurgeirsson, B.; Abe, M.; Baker, D.R.; Konno, P.; Haemmerle, S.; Thurston, H.J.; Papavassilis, C.; Richards, H.B. *Br. J. Dermatol.* **2013**, *168*, 412. DOI: 10.1111/bjd.12110.
7. McInnes, I.B.; Mease, P.J.; Kirkham, B.; Kavanaugh, A.; Ritchlin, C.T.; Rahman, P.; van der Heijde, D.; Landewé, R.; Conaghan, P.G.; Gottlieb, A.B.; Richards, H.; Pricop, L.; Ligozio, G.; Patekar, M.; Mpofu, S. *Lancet*, **2015**, *386*, 1137. DOI: 10.1016/S0140-6736(15)61134-5.
8. Tabarkiewicz, J.; Pogoda, K.; Karczmarczyk, A.; Pozarowski, P.; Giannopoulos, K. *Arch. Immunol. Ther. Exp.* **2015**, *63*, 435. DOI: 10.1007/s00005-015-0344-z.
9. For reviews on the subject see:
(a) Dhar, T.G.M.; Zhao ,Q.; Markby , D.W. *Ann. Rep. Med. Chem.* **2013**, *48*, 169. DOI: 10.1016/B978-0-12-417150-3.00012-0.
(b) Bronner, S.M.; Zbieg, J.R.; Crawford, J.J. *Expert Opin. Ther. Pat.* **2017**, *27*, 101. DOI: 10.1080/13543776.2017.1236918.
(c) Tice, C.M.; Bukhtiyarov, Y.; Zheng, Y.J.; Lala , D.; Singh, S.B. *Med. Chem. Rev.* **2017**, *52*, 195. DOI: 10.29200/acsmedchemrev-v52.ch11.
(d) Pandya, V.B.; Kumar, S.; Sachchidanand; Sharma, R.; Desai, R.C. *J. Med. Chem.* **2018**, *61*, 10976. DOI: 10.1021/acs.jmedchem.8b00588.
For recent papers see:
(e) Duan, J.J.W. ; Lu, Z. ; Jiang, B. ; Stachura, S. ; Weigelt, C.A. ; Sack, J.S. ; Khan, J. ; Ruzanov, M. ; Galella, M.A. ; Wu, D.R. ; Yarde, M. ; Shen, D.R. ; Shuster, D.J. ; Borowski, V. ; Xie, J.H. ; Zhang, L. ; Vanteru, S. ; Gupta, A.K. ; Mathur, A. ; Zhao, Q. ; Foster, W. ; Salter-Cid, L.M. ; Carter, P.H. ; Dhar, T.G.M. *ACS Med. Chem. Lett.* **2019**, *10*, 367. DOI: 10.1021/acsmedchemlett.9b00010.
(f) Kotoku, M. ; Maeba, T. ; Fujioka, S. ; Yokota, M. ; Seki, N. ; Ito, K. ; Suwa, Y. ; Ikenogami, T. ; Hirata, K. ; Hase, Y. ; Katsuda, Y. ; Miyagawa, N. ; Arita, K. ; Asahina, K. ; Noguchi, M. ; Nomura, A. ; Doi, S. ; Adachi, T. ; Crowe, P. ; Tao, H. ; Thacher, S. ; Hashimoto, H. ; Suzuki, T. ; Shiozaki M. *J Med Chem.* **2019**, *62*, 2837. DOI: 10.1021/acs.jmedchem.8b01567.
(g) Tian, J. ; Sun, N. ; Yu, M. ; Gu, X. ; Xie, Q. ; Shao, L. ; Liu, J. ; Liu, L. ; Wang, Y. *Eur J Med Chem.* **2019**, *167*, 37. DOI: 10.1016/j.ejmech.2019.01.082.
(h) Gong, H. ; Weinstein, D.S. ; Lu, Z. ; Duan, J.J. ; Stachura, S. ; Haque, L. ; Karmakar, A. ; Hemagiri, H. ; Raut, D.K. ; Gupta, A.K. ; Khan, J. ; Camac, D. ; Sack, J.S. ; Pudzianowski, A. ; Wu, D.R. ; Yarde, M. ; Shen, D.R. ; Borowski, V. ; Xie, J.H. ; Sun, H. ; D'Arienzo, C. ; Dabros, M. ; Galella, M.A. ; Wang, F. ; Weigelt, C.A. ; Zhao, Q. ; Foster, W. ; Somerville, J.E. ; Salter-Cid, L.M. ; Barrish, J.C. ; Carter, P.H. ; Dhar, T.G.M. *Bioorg Med Chem Lett.* **2018**, *28*, 85. DOI: 10.1016/j.bmcl.2017.12.006.
(i) Wang Y. ; Cai W. ; Tang T. ; Liu Q. ; Yang T. ; Yang L. ; Ma Y. ; Zhang G. ; Huang Y. ; Song X. ; Orband-Miller L.A. ; Wu Q. ; Zhou L. ; Xiang Z. ; Xiang J.N. ; Leung S. ; Shao L. ; Lin X. ; Lobera M. ; Ren F. *ACS Med Chem Lett.* **2018**, *9*, 120. DOI: 10.1021/acsmedchemlett.7b00476.
(j) Sasaki Y. ; Odan M. ; Yamamoto S. ; Kida S. ; Ueyama A. ; Shimizu M. ; Haruna T. ; Watanabe A. ; Okuno T. *Bioorg Med Chem Lett.* **2018**, *28*, 3549. DOI: 10.1016/j.bmcl.2018.09.032.
(k) Carcache D.A. ; Vulpetti A. ; Kallen J. ; Mattes H. ; Orain D. ; Stringer R. ; Vangrevelinghe E. ; Wolf R.M. ; Kaupmann K. ; Ottl J. ; Dawson J. ; Cooke N.G. ; Hoegenauer K. ; Billich A. ; Wagner J. ; Guntermann C. ; Hintermann S. *J Med Chem.* **2018**, *61*, 6724. DOI: 10.1021/acs.jmedchem.8b00529.
(l) Fukase, Y. ; Sato, A. ; Tomata, Y. ; Ochida, A. ; Kono, M. ; Yonemori, K. ; Koga, K. ; Okui, T. ; Yamasaki, M. ; Fujitani, Y. ; Nakagawa, H. ; Koyama, R. ; Nakayama, M. ; Skene, R. ; Sang, B.C. ; Hoffman, I. ; Shirai J. ; Yamamoto, S. *Bioorg Med Chem.* **2018**, *26*, 721. DOI: 10.1016/j.bmc.2017.12.039.
(m) Shirai, J. ; Tomata, Y. ; Kono, M. ; Ochida, A. ; Fukase, Y. ; Sato, A. ; Masada, S. ; Kawamoto, T. ; Yonemori, K. ; Koyama, R. ; Nakagawa, H. ; Nakayama, M. ; Uga, K. ; Shibata, A. ; Koga, K. ; Okui, T. ; Shirasaki, M. ; Skene, R. ; Sang, B. ; Hoffman, I. ; Lane, W. ; Fujitani, Y. ; Yamasaki, M. ; Yamamoto, S. *Bioorg Med Chem.* **2018**, *26*, 483. DOI: 10.1016/j.bmc.2017.12.006.
(n) Kono, M. ; Oda, T. ; Tawada, M. ; Imada, T. ; Banno, Y. ; Taya, N. ; Kawamoto, T. ; Tokuhara, H. ; Tomata, Y. ; Ishii, N. ; Ochida, A. ; Fukase, Y. ; Yukawa, T. ; Fukumoto, S. ; Watanabe, H. ; Uga, K. ; Shibata, A. ; Nakagawa, H. ; Shirasaki, M. ; Fujitani, Y. ; Yamasaki, M. ; Shirai, J. ; Yamamoto, S. *Bioorg Med Chem.* **2018**, *26*, 470. DOI: 10.1016/j.bmc.2017.12.008.
10. Kumar, N.; Solt, L.A.; Conkright, J.J.; Wang, Y.; Istrate, M.A.; Busby, S.A.; Garcia-Ordonez, R.D.; Burris, T.P.; Griffin, P.R. *Mol. Pharmacol.* **2010**, *77*, 228. DOI: 10.1124/mol.109.060905.
11. OPLS3e, Schrödinger, Inc., New York, NY, 2013 and Shivakumar, D.; Harder, E.; Damm, W.; Friesner, R. A.; Sherman, W. *J. Chem. Theory Comput.* **2012**, *8*, 2553. DOI: 10.1021/ct300203w.
12. This reaction proceeds likely in two steps: formation of the enamino ester, then cyclization. It is believed that during the first plateau at 110°C, optimal formation of the enaminoester is occurring and that subsequent heating to 150°C is required for the cyclization to the quinoline ring.
13. Dodey, P.; Bondoux, M.; Houziaux, P.; Barth, M.; Ou, K. PCT Patent WO 97/07115.
14. Ekroos, M.; Sjögren, T. *Proc. Natl. Acad. Sci. USA* **2006**, *103*, 13682. DOI: 10.1073/pnas.0603236103.